

Chaos crisis and bistability of self-pulsing dynamics in a laser diode with phase-conjugate feedback

Martin Virte,^{*} Andreas Karsaklian Dal Bosco, Delphine Wolfersberger, and Marc Sciamanna
*Supélec, OPTEL Research Group, Laboratoire Matériaux Optiques, Photonique et Systèmes, EA-4423, 2 rue Edouard Belin,
 F-57070 Metz, France*

(Received 7 July 2011; published 21 October 2011)

A laser diode subject to a phase-conjugate optical feedback can exhibit rich nonlinear dynamics and chaos. We report here on two bifurcation mechanisms that appear when increasing the amount of light being fed back to the laser. First, we report on a full suppression of chaos from a crisis induced by a saddle-node bifurcation on self-pulsing, so-called external-cavity-mode solutions (ECMs). Second, the feedback-dependent torus and saddle-node bifurcations on ECMs may be responsible for large regions of bistability between ECMs of different and high (beyond gigahertz) frequencies.

DOI: [10.1103/PhysRevA.84.043836](https://doi.org/10.1103/PhysRevA.84.043836)

PACS number(s): 42.65.Sf, 05.45.-a, 42.60.Mi, 42.65.Hw

I. INTRODUCTION

Phase-conjugate optical feedback (PCF) has been extensively used for applications where one needs to stabilize a laser diode output through phase or mode locking [1,2] or to improve laser performances such as single-mode emission [3], spectral linewidth [4,5], and intensity noise [6]. However, experimental and theoretical works have shown that, depending on the feedback parameters, the laser diode also can exhibit complex nonlinear dynamics, leading to chaos [7–17]. To summarize, when increasing the feedback strength, the laser diode is destabilized from its otherwise steady-state dynamic and exhibits a sequence of bifurcations to chaos. Regions of chaos (also called “bubbles”) are interspersed by self-pulsing dynamics [12]. Because the oscillation frequency of these self-pulsations is close to a multiple of the external-cavity frequency, these solutions have been called external-cavity modes (ECM). An in-depth bifurcation analysis of these ECMs is, however, available only for weak optical feedback [15,16], where one can also benefit from approximations of the ECM solutions [8,11] and appropriate asymptotic methods [17]. Yet the experiments suggest that the laser spectral component at the external-cavity frequency increases and broadens with the increase of feedback strength, hence indicating that restabilization of ECM and/or additional bifurcations on ECMs may be in order for larger feedback rates (see, e.g., cases e to g of Fig. 3 in Ref. [14]). This situation contrasts with the case of conventional optical feedback, where a continuous increase of feedback strength typically leads to an even more developed chaos such as coherence collapse [18].

In this paper, we extend the previously reported bifurcation analysis to larger values of the feedback strength. Using both direct numerical integration and continuation tools for delay-differential equations, we unveil two bifurcation scenarios. First, when increasing the feedback strength, a full suppression of chaos may be observed because of a crisis from a saddle-node bifurcation on ECM. As a result, the laser diode is left in a purely regular self-pulsing dynamic with a frequency that is a multiple of the external-cavity frequency. Second, bistability between ECMs can appear when increasing the feedback strength and leads to coexisting self-pulsing dynamics of

very high frequencies (for our parameters, several tens of gigahertz). These results show a configuration where a laser regular self-pulsing dynamic gets stabilized by the increase of feedback rate other than the reported regular pulse package in conventional optical feedback [19,20] or polarization self-modulation and square waveforms in polarization rotated feedback [21,22].

The plan of our paper is as follows. In Sec. II we detail the theoretical model and parameters, and discuss the bifurcation results explaining chaos crisis when increasing the feedback strength. Section III illustrates bistability between self-pulsating dynamics at a frequency being a multiple of the external cavity frequency. Our conclusions are summarized in Sec. IV.

II. CHAOS CRISIS

We model the laser system using the so-called Lang-Kobayashi equations, i.e., time-delayed differential equations for the slowly varying optical field Y and the carrier inversion Z . The field dynamics accounts for a delayed and phase-conjugated feedback field Y^* . The model is written as follows, where the time scale has been normalized by the photon lifetime (as done in Ref. [17]):

$$\frac{dY}{dt} = (1 + i\alpha)ZY + \gamma Y^*(t - \theta), \quad (1)$$

$$T \frac{dZ}{dt} = P - Z - (1 + 2Z)|Y|^2. \quad (2)$$

In these equations γ is the normalized feedback rate, θ is the normalized external delay, α stands for the linewidth enhancement factor, P is the pump parameter above threshold, and T is defined as the ratio of carrier to photon lifetime. To simplify the comparison with previous works, we have taken the same values of the parameters as in Refs. [9,12,15–17]: $P = 0.0417$, $T = 1428$, $\alpha = 3$, $\theta = 476$. These are typical values of a diode laser working close to threshold and subject to feedback from a 10-cm-distant mirror. The normalized feedback rate γ is our bifurcation parameter and will be varied between 0 and 0.07, which correspond to external mirror reflectivities from 0% to 3.35%. The model is simple in that it does not account for the phase-conjugate mirror internal dynamic (typically on nanosecond to second time scales [23]) and the multiple delayed round-trips in the extended cavity

^{*}martin.virte@supelec.fr

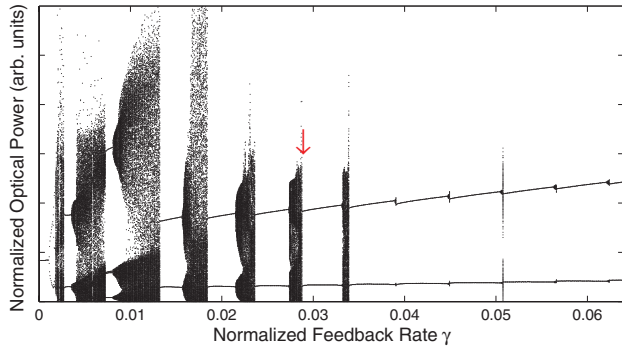


FIG. 1. (Color online) Bifurcation diagram for $\gamma \in [0, 0.07]$. The extrema of the time series of the optical power vs the normalized feedback rate are shown.

(which may occur in very strong feedback situations [24]). Still, it contains the main ingredients (ECMs and underlying bifurcations) to explain qualitatively the dynamics observed in experiments, and it allows for a mathematical treatment using either numerical bifurcation tools or asymptotic mathematical analysis.

Figure 1 shows a bifurcation diagram of the extrema of laser output power ($|Y|^2$) versus the feedback rate γ . One recognizes the sequence of bifurcations at weak feedback rate ($\gamma < 0.015$) as reported in Refs. [12,15,16]: the laser steady state destabilizes with a Hopf bifurcation to a ECM self-pulsing, which further undergoes a torus bifurcation to chaos. As the feedback rate increases, the parameter range where chaos is seen (i.e., the size of the bubbles of chaos) shrinks progressively until chaos disappears for larger feedback rate values. For $\gamma > 0.035$ the laser diode is left in a purely regular self-pulsing dynamic corresponding to an ECM solution of the laser system. When increasing the feedback rate, bifurcations between ECMs lead to successive jumps between self-pulsing solutions of different frequencies, all being multiples of the external-cavity frequency (i.e., a property of ECM solutions), but ECMs do not exhibit higher-order bifurcations to stable chaotic attractors.

To understand the mechanism leading to suppression of chaos, it is of interest to analyze in more detail the transition from chaos to ECM self-pulsing. The bifurcation diagram suggests an abrupt destabilization of chaos that is indicative of a crisis. This is confirmed in Fig. 2, where we plot time traces of laser output power and projections of the trajectory in the reduced phase space (real vs imaginary parts of the field) for $\gamma = 0.028795$, which is just before the transition from chaos to ECM self-pulsing indicated by the arrow in Fig. 1. In several time intervals of the chaotic time series (1.a) in Fig. 2, the laser diode exhibits a self-pulsing dynamic that resembles very much the dynamic of the next appearing ECM [see, e.g., a zoom in time series (2.a)]. This is also better seen in the phase space [Fig. 2, (1.b) and (2.b)] where one recognizes the limit cycle dynamic of the ECM as contained in the larger chaotic attractor. When increasing the feedback rate, the chaotic attractor born on an ECM grows in size until it starts exhibiting large trajectories, forming the ghost of the

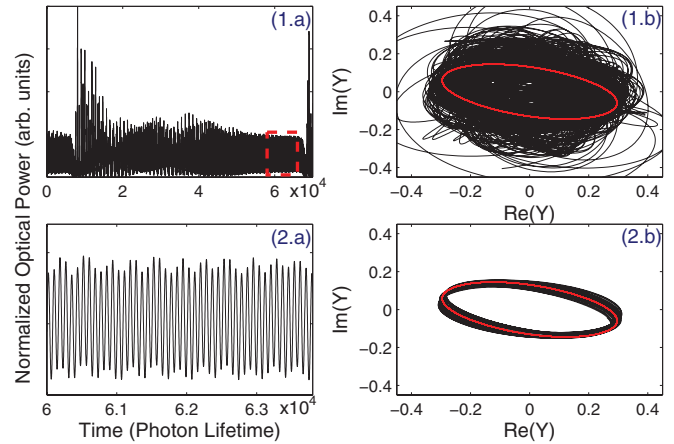


FIG. 2. (Color online) Time series of output power (1.a) and phase-space trajectory (1.b) for $\gamma = 0.028795$. Time series (2.a) is an enlargement of the boxed part, with (2.b) being its trajectory. In (1.b) and (2.b) the ellipse is the trajectory of the stable ECM about to appear.

limit-cycle trajectory of the next ECM, which is the signature of a so-called chaos crisis from a saddle-node bifurcation of a limit cycle (in our case an ECM solution). Such a crisis scenario, which happens for all bubbles of chaos starting from weak optical feedback, has been suggested also in Ref. [12], the originality being here to understand how the crisis combined with the saddle-node bifurcation on ECM may be responsible for a total disappearance of chaos for larger values of the feedback rate.

To answer this question, one has to get a closer look into the saddle-node bifurcation of the ECM and whether this bifurcation occurs for feedback rates smaller or larger than the torus bifurcation destabilizing the ECM and leading to chaos. We have then complemented our numerical study by mathematical continuation techniques using the DDE-BIFTOOL package [25]. It allows us to follow stable or unstable branches of steady states or time-periodic solutions and to analyze their linear stability. Figure 3 complements the previous bifurcation diagram by showing the branches of ECMs (only the maximum

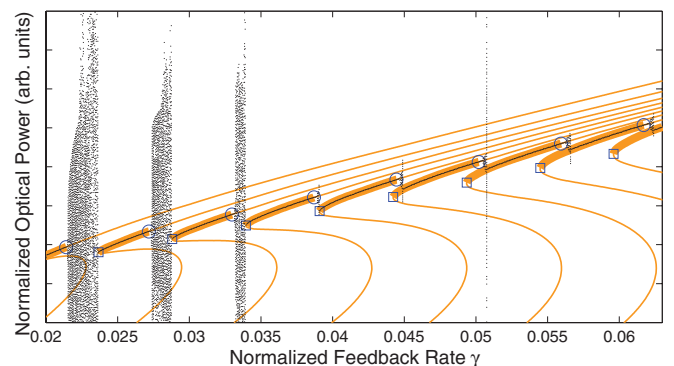


FIG. 3. (Color online) Bifurcation diagram obtained by the simulation and continuation method. The simulation result is in black, and the continuation result is in orange (gray). The stable part of the branch is a thick line, while the unstable part is a thin line. Squares (circles) are saddle-node (torus) bifurcations.

of $|Y|^2$ is plotted) that successively appear when increasing the feedback rate. The stable (unstable) part of each branch is displayed by a thick (thin) line. Each ECM is born from a saddle-node bifurcation (squares) where the high-intensity solution only can be stable. Each ECM then destabilizes with a torus bifurcation (circles) when increasing the feedback rate. The interval of feedback-rate values that separate the torus bifurcation of a previous ECM and the saddle-node bifurcation of the next ECM decreases as the feedback rate increases. Since the saddle-node bifurcation is responsible for the disappearance of chaos, this also explains that regions of chaos are observed for progressively smaller ranges of feedback rates as the feedback rate is increased. Furthermore, a sudden change of the bifurcation picture happens for $\gamma > 0.035$: the saddle-node bifurcation that creates the next stable ECM occurs for a feedback rate smaller than the torus bifurcation that destabilizes the previous ECM. As a result the mechanism inducing the chaos crisis is present as soon as the ECM gets destabilized, and chaos is no longer observed. This is a remarkable feature of the combination in our laser system of a chaos crisis mechanism and a bifurcation mechanism that makes the position of torus and saddle-node bifurcations on limit cycles dependent on the feedback rate. Control of chaos up to its full suppression is therefore rendered possible by varying the feedback strength.

III. BISTABILITY OF SELF-PULSING DYNAMICS

The bifurcation mechanism explained in Fig. 3 has another consequence: bistability can be observed between ECM solutions when increasing the feedback rate. Another mechanism leading to bistability of locked solutions in a laser diode with phase-conjugate feedback has been reported in Ref. [15], but as stated by the authors in a very small region of the parameters and with solutions having a small basin of attraction with respect to other stable attractors. As a result such a bistability was hardly observable in direct numerical integration and was seen only with the help of continuation methods where the system could be started with initial conditions in close

proximity to the coexisting solutions. In our case, not only is the bifurcation leading to bistability different, but also bistability is seen in a large interval of feedback rate values, an interval that moreover increases with the increase of the feedback rate. Bistability between ECMs is clearly seen in Fig. 4(a), where we plot the bifurcation diagrams of laser output power (only the maximum of $|Y|^2$ is plotted) for either increasing (top line) or decreasing (bottom line) feedback rates. We determine the boundaries of each region of bistability by looking at the feedback rate that corresponds to each saddle-node bifurcation (torus bifurcation) creating (destabilizing) an ECM. These boundaries are represented by pairs of vertical dashed lines. As we can see, all the states are easily accessible in the simulation, and the regions of bistability are quite large. In Fig. 4(b) we show the frequencies of the ECM solutions as they bifurcate when increasing the feedback rate. The frequency separation between ECMs is close to the external-cavity frequency. In our case the normalized external frequency is $f_{\text{ext}} = 1/\theta = 2.1 \cdot 10^{-3}$; hence it is about 1.5 GHz if one accounts for a photon lifetime of $\tau_p = 1.4$ ps as in Refs. [9,12,15,16]. To illustrate the coexistence of two ECM solutions with different and possibly high frequencies, we show in Fig. 5 the time series of the two regular self-pulsing dynamics observed for a normalized feedback rate of $\gamma = 0.0611$ [Figs. 5(a) and 5(b)] together with their corresponding optical spectra [Figs. 5(c) and 5(d)]. The zero frequency in Figs. 5(c) and 5(d) corresponds to the free laser frequency, which is the frequency reference frame of Eqs. (1) and (2). The optical spectrum in Fig. 5(c) [Fig. 5(d)] shows two peaks at about 8 (8.75) GHz and -8 (-8.75) GHz. Since the complex field trajectory is symmetric in the phase plane of the real vs imaginary parts and is centered on the (0,0) point, the optical spectrum shows no component at the zero frequency and symmetric peaks on negative and positive frequencies. Because one complete cycle for the complex field Y is equivalent to two cycles for $|Y|^2$, the time series of the optical power in Figs. 5(a) and 5(b) show modulations at about 16 and 17.5 GHz, respectively. The laser system will initially select one of the two coexisting self-pulsations at high frequencies. However a sustained perturbation or noise may induce random jumps between these two ECMs, with the result being a time-averaged rf spectral signature that is made of two peaks, slightly shifted in frequency (the shift is related to the external-cavity frequency). The observation of such robust self-pulsations at controllable (with the feedback rate) and high frequencies and moreover the possibility to observe bistability between these ECM solutions are of interest for all-optical signal processing.

Finally, we have checked the robustness of the reported bifurcation mechanism when varying the laser and feedback parameters. First, the increase of the linewidth enhancement factor does not modify the reported bifurcation scenario but increases the number and the size of the bubbles of chaos for weak optical feedback. Second, the reported findings are not specific to a so-called short external cavity. We still observe the feedback-induced suppression of chaos and ECM bistability when increasing the delay or the pump parameter such that the delay becomes larger than the free-running laser relaxation-oscillation frequency. The increase of the time-delay value, however, leads to additional bifurcations

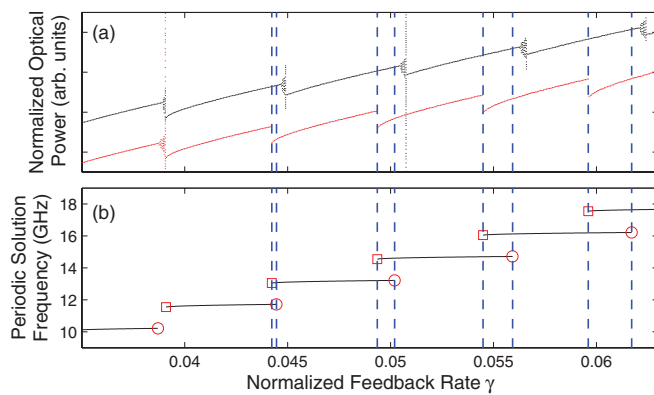


FIG. 4. (Color online) (a) Bifurcation diagram for increasing (top line) and decreasing feedback (bottom line) plotted on the same scale but shifted vertically for clarity. (b) The frequency of the periodic solutions (stable part only) obtained by continuation vs the normalized feedback rate. Dashed vertical lines bound the bistability regions.

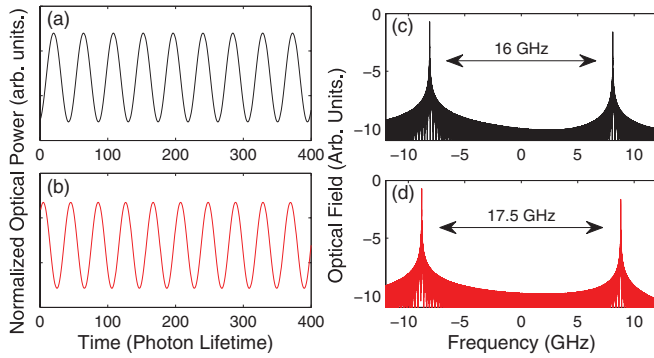


FIG. 5. (Color online) (a) and (b) Two time series of the light output power available for a normalized feedback rate of $\gamma = 0.0611$ and (c) and (d) the corresponding optical spectra.

on ECMs, which deserve further investigations. This conclusion contrasts strongly with the Conventional Optical Feedback (COF) case, where similar self-pulsing dynamics at the external-cavity (EC) frequency is typically limited to a so-called short external cavity [26]. This can be justified by the very different bifurcation mechanism leading to EC self-pulsing dynamics in both cases. In COF, the bifurcation mechanism is a Hopf bifurcation on an ECM, that is, a steady-state solution of the compound cavity system. The self-pulsing dynamics corresponds mathematically to a bridge of the time-periodic solution connecting two Hopf bifurcations on two frequency-detuned ECMs or, equivalently, to an ECM beating [27,28]. Moreover, as one of the connecting ECMs is typically an unstable solution (called antimode), the self-pulsing dynamics gets easily destabilized to, e.g., quasiperiodicity and chaos as one increases even slightly the feedback rate [29]. This makes the observation of such an ECM beating and Hopf bridge quite difficult. In the PCF case, the laser has only one stable steady-state solution, which gets destabilized through a Hopf bifurcation to a stable self-pulsing solution. As mentioned earlier, since the frequency of that solution is close to the external-cavity frequency, that solution has been called an ECM, but in contrast to COF, an ECM of the PCF system is a rotating solution with time-periodic intensity and is not a time-constant intensity. The laser creates such ECM solutions as the feedback increases, but all originate from the same single steady-state branch and not, as for the COF,

from a possible beating or Hopf bridge on (ECM) steady-state solutions. The stability of the EC self-pulsing dynamics in PCF (i.e., of the ECM solution) is determined by the interplay between a saddle-node bifurcation on the limit cycle and a torus bifurcation, hence making it possible to observe a robust and fully stable self-pulsing also when increasing the feedback rate or the external-cavity length.

IV. CONCLUSION

In summary, we have reported on a bifurcation scenario in a laser diode with phase-conjugate optical feedback. When increasing the feedback rate, the saddle-node bifurcation that creates a self-pulsating ECM solution (limit cycle) may occur for a feedback rate value smaller than the one corresponding to the torus bifurcation of another ECM. This results first in a full suppression of chaos for larger values of the feedback rate, where the underlying bifurcation mechanism is a crisis from a saddle-node bifurcation on the limit cycle. The laser then exhibits robust self-pulsating dynamics at frequencies being multiples of the external-cavity frequency, hence adjustable. Secondly, this leads to bistability between self-pulsating ECM solutions of different and high frequencies. The reported bifurcation scenarios are observed in a large range of parameters. These conclusions have been obtained through direct numerical integration of an appropriate set of rate equations and also from the use of advanced continuation tools for delay-differential equations. The reported dynamics are of interest for the all-optical generation of high-frequency microwave signals, and also the bistability is of interest for all-optical signal processing. Many of the reported bifurcation features, particularly the existence of a robust self-pulsing dynamics at large feedback rates, contrast with what is typically seen in a conventional optical feedback. They motivate further investigations in experiments where, although not detailed, reports show the existence of more regular attractors coexisting at large feedback rates.

ACKNOWLEDGMENTS

The authors acknowledge the support of Conseil Regional de Lorraine, Fondation Supélec, Institut Carnot C3S, and COST European Action MP0702.

-
- [1] L. Petersen, U. Gliese, and T. N. Nielsen, *IEEE J. Quantum Electron.* **30**, 2526 (1994).
 - [2] E. Miltenyi, M. O. Ziegler, M. Hofmann, J. Sacher, W. Elsaßer, E. O. Gobel, and D. L. MacFarlane, *Opt. Lett.* **20**, 734 (1995).
 - [3] M. Løbel, P. M. Petersen, and P. M. Johansen, *Opt. Lett.* **23**, 825 (1998).
 - [4] K. Vahala, K. Kyuma, A. Yariv, S.-K. Kwong, M. Cronin-Golomb, and K. Y. Lau, *Appl. Phys. Lett.* **49**, 1563 (1986).
 - [5] P. Kurz and T. Mukai, *Opt. Lett.* **21**, 1369 (1996).
 - [6] L. N. Langley and K. A. Shore, *Opt. Lett.* **18**, 1432 (1993).
 - [7] G. P. Agrawal and J. T. Klaus, *Opt. Lett.* **16**, 1325 (1991).
 - [8] G. H. M. van Tartwijk, H. J. C. van der Linden, and D. Lenstra, *Opt. Lett.* **17**, 1590 (1992).
 - [9] G. R. Gray, D. Huang, and G. P. Agrawal, *Phys. Rev. A* **49**, 2096 (1994).
 - [10] A. Murakami and J. Othsubo, *IEEE J. Quantum Electron.* **33**, 1825 (1997).
 - [11] W. A. van der Graaf, L. Pesquera, and D. Lenstra, *Opt. Lett.* **23**, 256 (1998).
 - [12] B. Krauskopf, G. R. Gray, and D. Lenstra, *Phys. Rev. E* **58**, 7190 (1998).
 - [13] O. Andersen, A. Fischer, I. Lane, E. Louvergneaux, S. Stolte, and D. Lenstra, *IEEE J. Quantum Electron.* **35**, 577 (1999).

- [14] J. S. Lawrence and D. M. Kane, *Phys. Rev. A* **63**, 033805 (2001).
- [15] K. Green, B. Krauskopf, and K. Engelborghs, *Phys. D* **173**, 114 (2002).
- [16] K. Green, B. Krauskopf, and I. J. Bifurcation, *Chaos* **13**, 2589 (2003).
- [17] T. Erneux, A. Gavrielides, K. Green, and B. Krauskopf, *Phys. Rev. E* **68**, 066205 (2003).
- [18] D. Lenstra, B. Verbeek, and A. Den Boef, *IEEE J. Quantum Electron.* **21**, 674 (1985).
- [19] T. Heil, I. Fischer, W. Elsaßer, and A. Gavrielides, *Phys. Rev. Lett.* **87**, 243901 (2001).
- [20] A. Tabaka, K. Panajotov, I. Veretennicoff, and M. Sciamanna, *Phys. Rev. E* **70**, 036211 (2004).
- [21] H. Li, A. Hohl, A. Gavrielides, H. Hou, and K. D. Choquette, *Appl. Phys. Lett.* **72**, 2355 (1998).
- [22] M. Sciamanna, F. Rogister, O. Deparis, P. Mégret, M. Blondel, and T. Erneux, *Opt. Lett.* **27**, 261 (2002).
- [23] D. H. DeTienne, G. R. Gray, G. P. Agrawal, and D. Lenstra, *IEEE J. Quantum Electron.* **33**, 838 (1997).
- [24] L. N. Langlely, K. A. Shore, and J. Mørk, *Opt. Lett.* **19**, 2137 (1994).
- [25] K. Engelborghs, T. Luzyanina, and G. Samaey, Department of Computer Science, Katholieke Universiteit Leuven, Tech. Rep. TW-330, 2002 (unpublished); Software available at [<http://twr.cs.kuleuven.be/research/software/delay/ddebiftool.shtml>].
- [26] A. Tager and K. Petermann, *IEEE J. Quantum Electron.* **30**, 1553 (1994).
- [27] D. Pieroux, T. Erneux, B. Haegeman, K. Engelborghs, and D. Roose, *Phys. Rev. Lett.* **87**, 193901 (2001).
- [28] M. Sciamanna, T. Erneux, F. Rogister, O. Deparis, P. Mégret, and M. Blondel, *Phys. Rev. A* **65**, 041801 (2002).
- [29] T. Erneux, A. Gavrielides, and M. Sciamanna, *Phys. Rev. A* **66**, 033809 (2002).